B-Raf^{V600E} and thrombospondin-1 promote thyroid cancer progression

Carmelo Nucera[a,b], Alessandro Porrello[c], Zeus Andrea Antonello[b], Michal Mekel[a], Matthew A. Nehs[a], Thomas J. Giordano[d], Damien Gerald[e], Laura E. Benjamin[e], Carmen Priolo[f], Efisio Puxeddu[g], Stephen Finn[f], Barbara Jarzab[h], Richard A. Hodin[a], Alfredo Pontecorvi[i], Vânia Nose[j], Jack Lawler[b], and Sareh Parangi[a,1]

[a]Thyroid Cancer Research Laboratory, Endocrine Surgery Unit, Massachusetts General Hospital, Harvard Medical School, Boston, MA 02214; [b]Division of Cancer Biology and Angiogenesis, Department of Pathology, Beth Israel Deaconess Medical Center, Harvard Medical School, Boston, MA 02215; [c]Institute for Genome Sciences and Policy, Duke University, Durham, NC 27710; [d]Department of Pathology, University of Michigan Medical School, Ann Arbor, MI 48109; [e]Department of Pathology, Beth Israel Deaconess Medical Center, Harvard Medical School, Boston, MA 02215; [f]Department of Medical Oncology, Dana-Farber Cancer Institute, Harvard Medical School, Boston, MA 02115; [g]Endocrinology Unit, Department of Medicine, University of Perugia, 06126 Perugia, Italy; [h]Department of Nuclear Medicine and Endocrine Oncology, Maria Skłodowska-Curie Memorial Cancer Center and Institute of Oncology, 44-100 Gliwice, Poland; [i]Endocrinology Unit, Catholic University Medical School "A. Gemelli", 00168 Rome, Italy; and [j]Endocrine Pathology, Department of Pathology, Brigham and Women's Hospital, Harvard Medical School, Boston, MA 02115

Communicated by Patricia K. Donahoe, Massachusetts General Hospital, Boston, MA, April 23, 2010 (received for review October 8, 2009)

Although B-Raf^{V600E} is the most common somatic mutation in papillary thyroid carcinoma (PTC), how it induces tumor aggressiveness is not fully understood. Using gene set enrichment analysis and in vitro and in vivo functional studies, we identified and validated a B-Raf^{V600E} gene set signature associated with tumor progression in PTCs. An independent cohort of B-Raf^{V600E}-positive PTCs showed significantly higher expression levels of many extracellular matrix genes compared with controls. We performed extensive in vitro and in vivo validations on thrombospondin-1 (TSP-1), because it has been previously shown to be important in the regulation of tumor angiogenesis and metastasis and is present in abundance in tumor stroma. Knockdown of B-Raf^{V600E} resulted in TSP-1 downregulation and a reduction of adhesion and migration/invasion of human thyroid cancer cells. Knockdown of TSP-1 resulted in a similar phenotype. B-Raf^{V600E} cells in which either B-Raf^{V600E} or TSP-1 were knocked down were implanted orthotopically into the thyroids of immunocompromised mice, resulting in significant reduction in tumor size and fewer pulmonary metastases from the primary carcinoma as compared with the control cells. Treatment of orthotopic thyroid tumors, initiated 1 week after tumor cell implantation with PLX4720, an orally available selective inhibitor of B-Raf^{V600E}, caused a significant tumor growth delay and decreased distant metastases, without evidence of toxicity. In conclusion, B-Raf^{V600E} plays an important role in PTC progression through genes (i.e., TSP-1) important in tumor invasion and metastasis. Testing of a patient's thyroid cancer for B-Raf^{V600E} will yield important information about potential tumor aggressiveness and also allow for future use of targeted therapies with selective B-Raf^{V600E} inhibitors, such as PLX4720.

extracellular matrix | metastasis | papillary thyroid cancer | tumor microenvironment | cell invasion

Papillary thyroid cancer (PTC), with its incidence increasing by almost 5% each year, currently ranks as the eighth most common malignancy diagnosed in women (1). Neck recurrences alone are responsible for a third of thyroid cancer–related deaths. There is no effective treatment for radioiodine-resistant metastatic disease; the 10-year survival rate in these cases is only 10% (2). Molecular understanding of the aggressive clinical behavior of this subset of patients is needed to develop new therapeutic options.

The T1799A (V600E) point mutation occurs in exon 15, which encodes the kinase activation domain of B-Raf. It is the most prevalent genetic alteration implicated in the initiation and progression of PTC, especially in aggressive subtypes such as the tall cell variant of PTC and in those with extrathyroidal extension (3, 4) and lymph node or distant metastases (3, 5). It has been associated with both radioactive iodine refractoriness and PTC recurrence (3). The B-Raf^{V600E} mutation possesses elevated kinase activity that leads to activation of the MAPK (i.e., ERK1/2) signaling pathway (6). Although it is not clearly understood how B-Raf^{V600E} mutation leads to more aggressive PTCs, some altered pathways have been previously described (3).

In our study, we analyzed the role of the B-Raf^{V600E} mutation in the expression and regulation of human genes linked to cell adhesion, migration, invasion, and metastasis. Gene set enrichment analysis (GSEA) was performed on microarray data from human PTCs with or without B-Raf^{V600E} mutation, as well as from human normal thyroid tissue (NT) samples. GSEA is a bioinformatic tool based on genome-wide expression profile analysis (7). It is based on the identification of gene set leading-edge genes that represent a subset of highly ranking genes mostly associated with detected differences between two experimental groups (7). We analyzed microarray data (8) to identify groups of genes (gene sets) significantly associated with B-Raf^{V600E} PTC that are regulated together, share the same function, or belong to the same biochemical pathway.

Using both in vitro and in vivo models of human thyroid cancer, we found that thrombospondin-1 (TSP-1), a multifunctional molecule known to have important effects on tumor stroma and endothelium, serves as a mediator of invasiveness and aggressive tumor behavior when the B-Raf^{V600E} mutation is present.

Results

GSEA was performed on microarray data (8) from 26 human PTCs with B-Raf^{V600E} mutation, 14 without B-Raf^{V600E} mutation, and 10 NT samples. Of 539 independent gene sets tested, 18 were significantly associated with PTCs-B-Raf^{V600E} mutation; 17 of these were up-regulated (including many genes important for the tumor microenvironment), and 1 was down-regulated (including genes involved in oxidative enzymatic reactions and cell polarity in epithelial cells), with a false-discovery rate (FDR) of <0.20. Details about gene sets associated with B-Raf^{V600E}-positive human PTCs and validation of the leading-edge genes using an independent cohort of PTCs, with or without B-Raf^{V600E} mutation, and NT are reported in *SI Text*, Figs. S1 and S2, and Tables S1 and S2.

Detailed validation was undertaken for gene sets enriched in leading-edge genes known to be important in angiogenesis, invasion, and metastasis. One such gene, TSP-1, was shown to be

Author contributions: C.N., J.L., and S.P. designed research; C.N., Z.A.A., M.M., M.A.N., T.J.G., D.G., C.P., E.P., and B.J. performed research; T.J.G. and L.E.B. contributed new reagents/analytic tools; C.N., Z.A.A., A. Porrello, D.G., S.F., R.A.H., A. Pontecorvi, V.N., J.L., and S.P. analyzed data; and C.N. wrote the paper.

The authors declare no conflict of interest.

[1]To whom correspondence should be addressed. E-mail: sparangi@partners.org.

This article contains supporting information online at www.pnas.org/lookup/suppl/doi:10.1073/pnas.1004934107/-/DCSupplemental.

significantly altered in PTCs with B-Raf^{V600E} mutation as part of the leading-edge of the BREAST_CANCER_ESTROGEN_SIGNALLING up-regulated gene set (Fig. S1 and Tables S1 and S2).

TSP-1 became the focus of our study because it (*i*) is a multifunctional matricellular protein (structured with amino- and carboxy-terminal domains and three types of sequence repeats) that regulates extracellular matrix (ECM) structure during tissue genesis and tumor progression (9, 10); (*ii*) binds concurrently to a wide variety of integrins (involved in cellular proliferation pathways and metastasis) and nonintegrin (i.e., proteoglycans) cell surface receptors, matrix proteins (i.e., fibronectin), cytokines (i.e., TGF-β1), proangiogenic factors (e.g., VEGF), and matrix proteases [i.e., matrix metalloproteinase (MMP)-9], indicating its importance in cross-talk between surface receptors; and (*iii*) serves as a key regulator of tumor cell adhesion and migration, metastasis, and angiogenesis and may direct clustering of receptors to specialized domains for these biological processes (9, 10).

TSP-1 Expression Is Regulated by B-Raf^{V600E} in 8505c Cells. The 8505c cell line is an authenticated human papillary/anaplastic thyroid carcinoma (*SI Text*), which was confirmed to harbor a V600E mutation (11). Greater than 90% B-Raf^{V600E} mRNA and protein levels silencing was achieved using two shRNAs (sh)—sh#1 and sh#10 targeting B-Raf^{V600E} (Fig. 1 *A* and *B*). This silencing resulted in significant down-regulation of phospho-MEK1/2 and phospho-ERK1/2, downstream of B-Raf^{V600E} kinase activity (Fig. 1*B*), as well as significant decrease in TSP-1 mRNA and protein levels (Fig. 1 *B–D*).

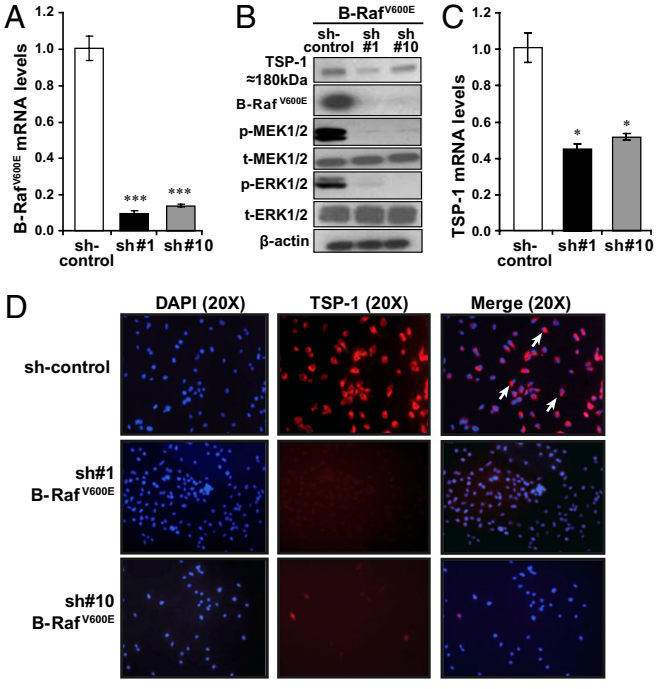

Fig. 1. TSP-1 expression in B-Raf^{V600E}-positive 8505c cells. (*A*) Real-time RT-PCR analysis in 8505c cells demonstrates a significant decrease of B-Raf^{V600E} relative mRNA levels by sh#1 [fold change (FC) =0.1 ± 0.01] and sh#10 (FC = 0.14 ± 0.007) vs. control (fold change = 1 ± 0.06). (*B*) Western blot analysis demonstrating a decrease greater than 90% of B-Raf^{V600E} protein levels by sh#1 and sh#10. B-Raf^{V600E} knockdown reduces endogenous levels of phosphorylated p-MEK1/2 (Ser217/221) and p-ERK1/2 (Thr202/Tyr204). Upon B-Raf^{V600E} silencing, TSP-1 protein levels are approximately 65% down-regulated by sh#1 and 50% by sh#10 upon B-Raf^{V600E} silencing vs. sh control 8505c cells. (*C*) Real-time RT-PCR analysis shows that TSP-1 relative mRNA levels are down-regulated approximately 2-fold by sh#1 (FC = 0.45 ± 0.03) and by sh#10 (FC = 0.51 ± 0.01). (*D*) Indirect immunofluorescence confirms that TSP-1 protein is down-regulated by sh#1 and sh#10 vs. sh control 8505c cells. These data represent the mean ± SEM of three independent experiments. *$P < 0.05$; ***$P < 0.001$.

Silencing of B-Raf^{V600E} in 8505c Cells Results in Decreased Proliferation, Adhesion, Migration, and Invasion. Silencing of B-Raf^{V600E} in 8505c thyroid cancer cells decreased BrdU (marker of cell proliferation) incorporation from 50.1% ± 5.1% in the controls to 35.6% ± 2.6% ($P < 0.05$) and 30.3% ± 2.5% ($P < 0.01$) by sh#1 and sh#10, respectively (Fig. 2*A*). There was also a reduction in the fraction of cells in S-phase from 43.5% ± 1.1% to 36.4% ± 3.3% (sh#1, $P < 0.01$) and 32.1% ± 1.3% (sh#10, $P < 0.001$), and an increase in G1 from 38.4% ± 1.6% in control 8505c cells to 49.3% ± 5.2% ($P < 0.01$) by sh#1 and 57.7% ± 3.5% ($P < 0.01$) by sh#10. B-Raf^{V600E} silencing did not lead to apoptosis (absence of sub-G1 cell population) according to flow cytometric analysis.

We found sh control 8505c cells to possess significant adhesive properties (97 ± 1.4 cells per field) on type I collagen after 2 h of incubation. By contrast, 8505c cells with B-Raf^{V600E} silenced by sh#1 (22.2 ± 3.8 cells per field, $P < 0.001$) and sh#10 (26.2 ± 3.0 cells per field, $P < 0.001$) showed a consistent and statistically significant reduction of adhesion (Fig. 2*B*).

B-Raf^{V600E} silencing by sh#1 and sh#10 unequivocally reduced migration of 8505c cells on type I collagen and invasion into Matrigel. Migration was reduced by approximately 3-fold (from 76 ± 5.6 to 25.2 ± 2.5 cells per field by sh#1 and to 27 ± 3.3 cells per field by sh#10, $P < 0.001$) and invasion by >20-fold (from 69 ± 4.2 to 3.5 ± 1.2 cells per field by sh#1 and to 3.2 ± 0.9 cells per field by sh#10, $P < 0.001$) (Fig. 2*C*). Conversely, WT B-Raf silencing in the papillary human thyroid carcinoma cell line TPC-1, which harbors a receptor tyrosine kinase translocation (RET/PTC-1) did not affect TSP-1 mRNA levels nor cellular proliferation, adhesion, migration, or invasion (*SI Text*).

TSP-1 Silencing Results in Decreased Proliferation, Adhesion, Migration, and Invasion of 8505c Cells. TSP-1 silencing using two sh resulted in 90% (sh#7) and 75% (sh#8) reduction of TSP-1 mRNA and protein expression levels (Fig. 3*A*), as well as a 60% reduction in phospo-ERK1/2 levels (Thr202/Tyr204) (Fig. 3*A*). TSP-1 silencing also decreased BrdU incorporation (from 50.0% ± 5.2% in controls to 13.7% ± 1.4% by sh#7, $P < 0.001$) (Fig. 3*B*); a reduction of the fraction of cells in S-phase from 43.5% ± 1.1% to 33.1% ± 5.6% by sh#7 ($P < 0.05$) was seen, as well as an increase of cells in G1 from 38.4% ± 1.6% in controls to 44.8% ± 0.1% ($P < 0.01$). TSP-1 silencing did not lead to apoptosis (absence of sub-G1 cell population), as demonstrated using flow cytometric

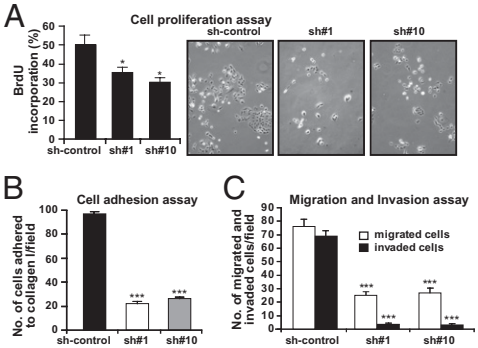

Fig. 2. Silencing of B-Raf^{V600E} and functional effects in 8505c cells. (*A*) Flow cytometry analysis shows a significant reduction of BrdU incorporation of 8505c cells B-Raf^{V600E} sh#1 and sh#10 in S-phase vs. sh control cells. (*B*) Cell adhesion and (*C*) migration and invasion assays show that B-Raf^{V600E} knockdown by both sh#1 and sh#10 significantly reduces the number of cells that adhered to type I collagen and the number of migrating and invading 8505c cells. These data represent the average ± SD of three independent experiments. *$P < 0.05$; ***$P < 0.001$.

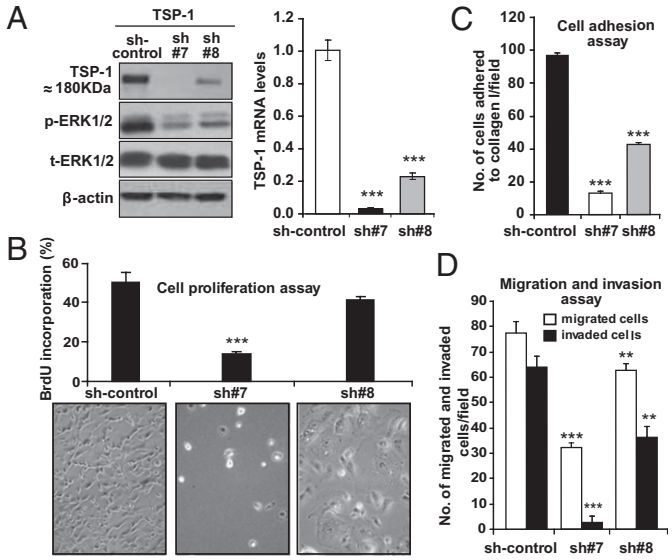

Fig. 3. TSP-1 silencing and functional effects in 8505c cells. (*A*) Western blot analysis shows a decrease in TSP-1 protein levels by shRNAs (sh) targeting TSP-1 in 8505c cells. TSP-1 knockdown reduces endogenous levels of phosphorylated p-ERK1/2 (Thr202/Tyr204). Real-time RT-PCR analysis shows a significant decrease of TSP-1 relative mRNA levels, 33.3-fold less by sh#7 [fold change (FC) = 0.03 ± 0.006] and 6.25-fold less by sh#8 (FC = 0.2 ± 0.013) vs. sh control cells (FC = 1.04 ± 0.1). (*B*) Flow cytometric analysis shows a significant reduction of BrdU incorporation in S-phase in 8505c cells sh#7 TSP-1 vs. sh control cells. (*C*) Cell adhesion and (*D*) migration and invasion assays show that knockdown of TSP-1 by both sh#7 and sh#8 significantly reduces the number of 8505c cells adherent to type I collagen substrate and the number of migrating and invading 8505c cells. These data represent the average ± SD of three independent experiments. $^{**}P < 0.01$; $^{***}P < 0.001$.

analysis. TSP-1 mRNA silencing in 8505c cells reduced tumor cell adhesion, migration, and invasion (Fig. 3 *C* and *D*).

The 8505c thyroid cancer cells treated with sh targeting TSP-1 showed a decrease in the number of cells that adhered to type I collagen compared with control levels (97 ± 1.4 cells per field in controls vs. 13 ± 2.1 cells per field by sh#7 and 42.5 ± 5.2 cells per field by sh#8, $P < 0.001$) (Fig. 3*C*). TSP-1 silencing also reduced migration on type I collagen and invasion into Matrigel. Migration was reduced from 77.2 ± 4.9 to 25.2 ± 2.5 (sh#7, $P < 0.001$) and 62.5 ± 2.8 cells per field (sh#8, $P < 0.01$) (Fig. 3*D*). Invasion was reduced from 64 ± 4.1 to 2.7 ± 2.5 by sh#7 and to 36.2 ± 4.5 cells per field by sh#8 ($P < 0.001$) (Fig. 3*D*). Similar results were obtained with an additional authenticated human papillary thyroid carcinoma cell line (i.e., BCPAP) harboring the V600E mutation (*SI Text* and Fig. S3) (11). To confirm the role of B-Raf^{V600E} in cell adhesion, migration, and invasion, we stably overexpressed B-Raf^{V600E} in normal human foreskin BJ fibroblasts. B-Raf^{V600E} overexpression in BJ cells was found to increase cell adhesion, migration, and invasion, as well as TSP-1 and phospho-ERK1/2 levels (*SI Text* and Fig. S4 *A* and *B*).

Proinvasive Role of B-Raf^{V600E} in 8505c Cells Is Mediated by TSP-1. To provide further mechanistic insight into the link between B-Raf^{V600E} and TSP-1, we assayed the behavior of 8505c thyroid cancer cells in a reconstituted 3D cell culture-based ECM assay in the presence of 5% FBS (*SI Text* and Figs. S5 *A–D* and S6*A*). In this assay, 8505c cells with B-Raf^{V600E} mutation showed invasive properties (dendritic-like morphology with filopodia-like structures) and high growth rate (large cell aggregates) (*SI Text* and Fig. S5 *A–D*). The invasive properties disappeared and the cells organized as small spheroids with knockdown of B-Raf^{V600E} or TSP-1 (Fig. 4 *B* and *C* and Figs. S5 *A–D* and S6*A*). Different stable protein components of TSP-1 (Fig. 4*A*), including amino-terminal domain [thought to be important in cell adhesion/migration through α3β1 (ITGA3B1) and α6β1 (ITGA6B1) integrin-binding domains], 3TSR (type I repeats known to be important in angiogenesis through the CD36), and carboxy-terminal domain (also important in cell adhesion and migration) were then added to the 8505c cells to determine whether the invasive phenotype could be rescued (Fig. 4 *B* and *C* and Fig. S6 *B–D*). Addition of 0.6 μM full-length human TSP-1 protein (Fig. 4*B*) or 2 μM of recombinant versions of the amino-terminal domain significantly restored the invasive phenotype in 8505c cells with B-Raf^{V600E} knockdown in this 3D Matrigel assay (Fig. 4*B* and Fig. S6*C*). Treated cells increased their growth rate and transformed to a dendritic-like morphology by day 9 (Fig. 4*B* and Fig. S6*C*). Treatment with 3TSR caused a slight reversion of the invasive phenotype (Fig. 4*B* and Fig. S6*C*). The 8505c cells with TSP-1 knockdown also transformed to a dendritic-like morphology upon the addition of amino-terminal or 3TSR domains (Fig. 4*C* and Fig. S6*D*). Treatment with the carboxy-terminal domain did not revert the morphology to the control phenotype for either B-Raf^{V600E} or TSP-1 knockdown cells (Fig. 4 *B* and *C* and Fig. S6 *C* and *D*). Together, these results indicate that

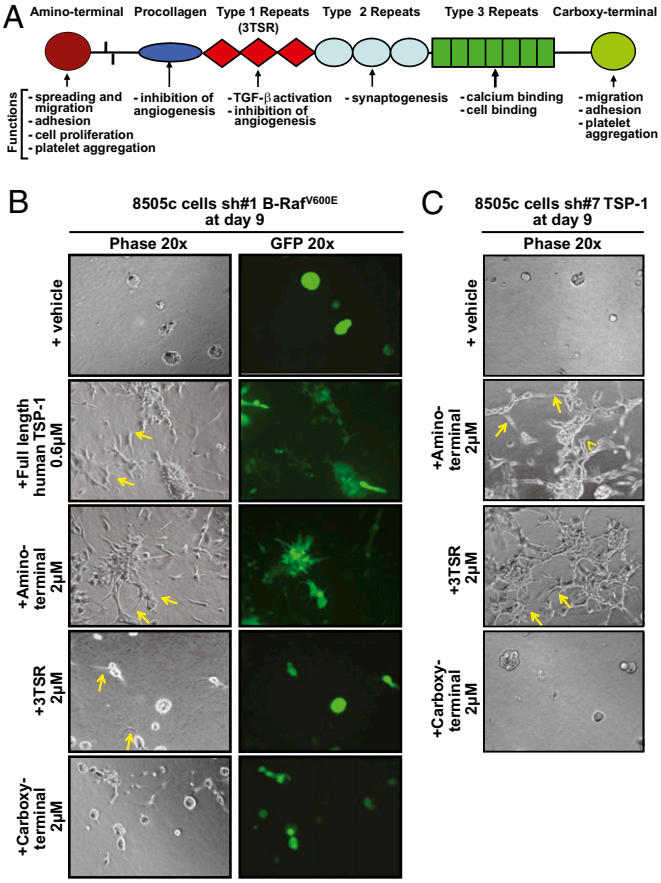

Fig. 4. Proinvasive role of B-Raf^{V600E} in 8505c cells grown in 3D cultures. (*A*) Structural and functional domains of full-length human TSP-1 protein. A single subunit is depicted as a series of structural domains based on the amino acid sequence. The vertical lines that are adjacent to the amino-terminal domain are the interchain disulfide bonds. (*B*) 3D cell culture–based ECM assay shows that treatment with 0.6 μM full-length human TSP-1 protein or 2 μM of recombinant amino-terminal domain of TSP-1 protein rescues the invasive phenotype (dendritic-like structures with filopodia; arrows) of 8505c cells that underwent knockdown of B-Raf^{V600E} (sh#1) (day 9). (*C*) 3D assay shows that treatment with 2 μM of recombinant amino-terminal or 3TSR domains of TSP-1 rescues the invasive phenotype (dendritic-like structures with filopodia; arrows) of 8505c cells with that underwent TSP-1 knockdown (sh#7) (day 9).

B-Raf^{V600E} 8505c thyroid cancer cells have higher potential for invasion and dissemination than 8505c cells with knockdown of either B-Raf^{V600E} or TSP-1. Amino-terminal and 3TSR domains of TSP-1 may cooperate mechanistically through a positive feedback with B-Raf^{V600E} in 8505c cells to activate ERK1/2 to p-ERK1/2 and promote tumor invasion and metastases.

Knockdown of Either B-Raf^{V600E} or TSP-1 Decreases Cell Growth and Metastasis in Vivo. Given our in vitro data, we wanted to evaluate the role of mutant B-Raf^{V600E} and TSP-1 in tumor growth and metastasis in vivo. We previously developed an orthotopic mouse model using 0.5×10^6 8505c human thyroid cancer cells in SCID mice (12). In this orthotopic model [Green Fluorescent Protein (GFP) engineered], all mice reliably developed palpable thyroid carcinomas by 5 weeks after injection of 8505c cells into the right thyroid, and necropsy showed large (Fig. 5*Bi–iii*) and highly proliferative (Fig. S7*A*) thyroid tumors with tracheal compression similar to the behavior of aggressive human thyroid carcinoma (Fig. 5*Bi–vi*). All sh control 8505c tumor-bearing mice had multiple histologically confirmed micrometastases to lungs (also visible by detection of GFP signal in vivo) (Fig. 5 *Aii* and *Ci–iii*). Fifty percent (3 of 6) of the sh control 8505c control mice had cervical lymph node metastasis (12). Orthotopic tumor-bearing mice were never found to have bone or liver metastases.

Here implantation of 8505c cells with knockdown of B-Raf^{V600E} (sh#1) into the right thyroid resulted in significantly smaller thyroid tumors at 5 weeks, with no evidence of cervical lymph node metastasis [mean orthotopic tumor volume was 0.50 ± 0.20 mm^3 ($n = 6$) vs. 350.1 ± 90 mm^3 for control tumor ($n = 6$) ($P < 0.001$)] (Fig. 5 *Ai* and *Bvii–xii*). Importantly, in those animals implanted with 8505c cells with B-Raf^{V600E} knockdown, the number of metastasis to the lungs from the primary orthotopic carcinoma was reduced from 18.5 ± 1 metastases per section of whole lung for the control tumors to 2 ± 0.8 metastases per section of whole lung for those with B-Raf^{V600E} knockdown (Fig. 5 *Aii* and *Civ–vi*). Implantation of 8505c cells with TSP-1 knockdown (sh#7) also produced significantly smaller tumors at 5 weeks (mean tumor volume was 15.1 ± 2.8 mm^3, $P < 0.001$) (Fig. 5 *Ai* and *Bxiii–xiv*) when compared with control, with fewer metastases (7.75 ± 1.15 metastases per section of whole lung for the 8505c tumors with TSP-1 knockdown compared with control, $P < 0.001$) (Fig. 5 *Aii* and *Cvii–viii*). In addition, proliferative rate, as measured by Ki-67 nuclear expression, was slightly lower in the small orthotopic carcinomas from 8505c cells in which either B-Raf^{V600E} or TSP-1 was knocked down (Fig. S7 *B* and *C*). Finally, given the known importance of TSP-1 to angiogenesis, we analyzed some angiogenic markers (e.g., CD31, VEGF, and MMP-2 and -9) in these tumors at 5 weeks after tumor implantation (*SI Text* and Fig. S7 *D–I*).

PLX4720 Inhibits Tumor Growth and Lung Metastasis in Vivo. Immunocompromised mice ($n = 16$) were orthotopically implanted with 8505c B-Raf^{V600E} human thyroid cancer cells, and 1 week after injection half were randomized to treatment with an orally absorbed compound PLX4720 (Plexxikon) that selectively inhibits B-Raf^{V600E} kinase activity (13). PLX4720 binds in the cleft between the N and C lobes of the B-Raf^{V600E} kinase domain near the hinge region, which overlaps with the ATP-binding site (13). PLX4720 treatment by oral gavage (30 mg/kg per day for 21 days) caused a significant reduction in tumor growth (>90%, $P < 0.001$) compared with control mice treated with vehicle, and dramatically decreased lung metastases (Fig. 5*D*), from 16 metastases per section of whole lung in the control group to 2 metastases per section of whole lung ($P < 0.001$), with no evidence of toxicity.

Discussion

Patients with B-Raf^{V600E}-positive PTCs have a higher risk of recurrent and persistent disease and a less favorable outcome (3, 14). In this study, we identified the gene expression signature of B-Raf^{V600E} by applying GSEA to microarray data from human PTCs with and without BRAF mutation. The B-Raf^{V600E} signature was validated in another independent cohort of human PTCs samples with comparisons performed in WT B-Raf PTCs, mutant B-Raf PTCs, or NT samples. Previous gene expression profiling studies on the effect of B-Raf^{V600E} focused on identifying individual genes that were up- or down-regulated in melanoma (15) and thyroid cancer (8). Although useful, they fail to detect biological processes affecting sets of genes that act in concert, such as metabolic or oncogenic pathways, which are distributed across an entire network of genes but are subtle at the level of individual genes (7). GSEA is a recent bioinformatic approach to genome-wide expression profiling that evaluates microarray data at the level of gene sets instead of single genes and overcomes some important limitations of traditional differential gene expression analysis (7).

In our GSEA analysis, B-Raf^{V600E} PTCs identified only one down-regulated gene set, which included genes involved in cell polarity in epithelial cells, thus suggesting B-Raf^{V600E}'s importance in cell dedifferentiation, loss of cell polarity, and tissue morphogenesis. We identified 17 up-regulated gene sets significantly associated with B-Raf^{V600E} in PTCs, including mainly those genes involved in the regulation of the tumor ECM, such as TSP-1, TGF-β1, ITGA3, ITGA6, ITGB1, FN, CD44, CTS-B, and CTS-S, which are identified as potential genes either targeted or affected by the B-Raf^{V600E} mutation in PTCs. These genes may act in concert and elicit important biological crosstalk and regulate the tumor microenvironment.

The role of B-Raf^{V600E} in tumor progression has been previously demonstrated in melanoma tumor cells (16, 17). To determine whether B-Raf^{V600E} could affect ECM composition and drive thyroid cancer progression, we validated various genes linked to invasion and metastasis and focused our in vitro and in vivo validations on TSP-1. TSP-1 and its target TGF-β1 are crucial regulators of epithelial cell growth, motility, polarity, and morphogenesis (9, 10) and are important in stromal/epithelial interaction and angiogenesis. Whereas the role of TSP-1 as an inhibitor of tumor angiogenesis is well documented, its biological action in tumor progression and metastasis requires further study (9, 10). In this study, TSP-1 was significantly increased in B-Raf^{V600E}-PTCs vs. NT and compared with WT B-Raf PTCs.

In our study, the results of B-Raf^{V600E} knockdown in 8505c cells indicate that this mutant caused increased cell proliferation, adhesion, migration, and invasion. We also found a significant though not complete decrease in TSP-1 mRNA and protein levels in the cells with B-Raf^{V600E} silencing, thus suggesting that this oncogene can affect TSP-1 levels by either transcriptional or posttranscriptional regulation.

TSP-1 knockdown in 8505c cells resulted in decreased phospho-ERK1/2 protein levels and reduced cell adhesion, migration, and invasion, as well as cell proliferation. In addition, the G1 arrest demonstrates that this protein promotes cell cycle progression. A number of studies have previously shown that TSP-1 is a mitogen-inducible immediate–early response gene (18) and is intimately involved in the regulation of cellular proliferation through effects on integrin pathways (19). Furthermore, consistent with our results, TSP-1 has been shown to be involved in the integrin pathways that can affect tumor cell adhesion (20) or migration/invasion (9).

There are few previous data on the role of TSP-1 in thyroid cancer progression and no previous studies demonstrating a link to B-Raf mutations. TSP-1 is able to enhance follicular thyroid cancer cell invasion by an increase of urokinase expression (21). In corroboration with a potential role of TSP-1 in thyroid cancer progression, microarray analysis of poorly differentiated or undifferentiated thyroid cancer subtypes has recently revealed up-regulation of TSP-1 in these aggressive human thyroid cancers; however, neither in vitro nor in vivo functional validations for TSP-1 were performed, nor was there any attempt to make a link to B-Raf mutation status in this study (22).

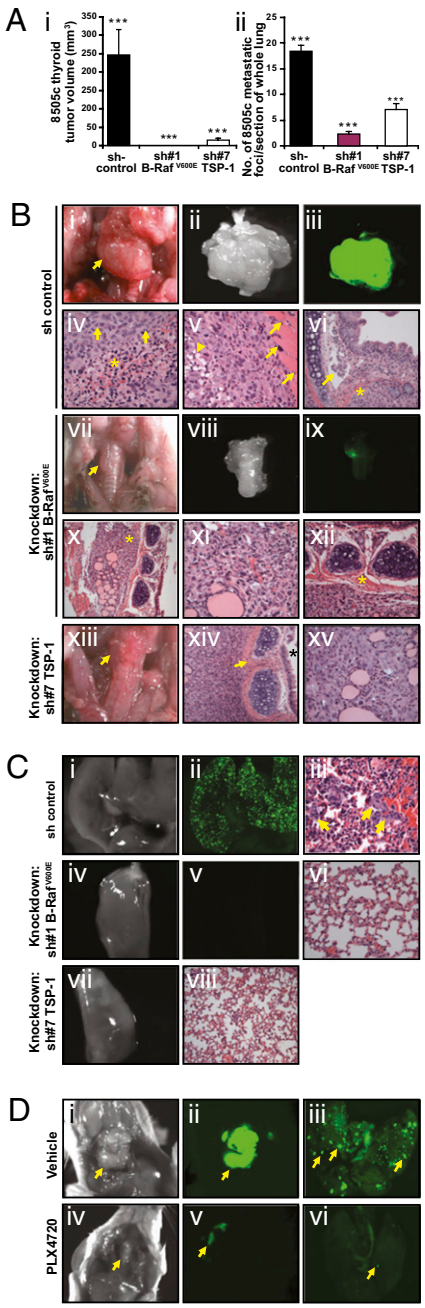

Fig. 5. Knockdown of either B-Raf^{V600E} or TSP-1 in an in vivo model of thyroid carcinoma. (*Ai*) Volume of orthotopic thyroid carcinomas (OTC) formed by sh control 8505c cells, sh#1 B-Raf^{V600E} cells, or sh#7 TSP-1 8505c cells. (*Aii*) Number of metastatic 8505c cells foci found in each mouse that was averaged per group ($n = 6$). These data represent the average ± SEM. (*Bi-iii*) Gross images of a large OTC (arrow) of sh control 8505c cells. (Magnification, ×10.) *Bii* (phase contrast) and *Biii* (GFP excitation): tracheal impingement. (*Biv–vi*) Histological sections (H&E). (*Biv*) OTC within the right thyroid, showing histopathologic features of a high-grade neoplasm: mitoses (arrows), necrosis (asterisk), and marked cellular pleomorphism. (Magnification: ×40.) (*Bv*) OTC invading the neck muscles (arrows) and fat (arrowhead). (Magnification: ×40.) (*Bvi*) adjacent tracheal wall (asterisk) and blood vessels (arrow). (Magnification: ×60.) (*Bvii–ix*) Gross image of an sh#1 8505c cells small OTC (arrow). (Magnification: ×10.) *Bviii*: phase contrast; *Bix*: GFP excitation. (*Bx* and *Bxi)* Small OTC (asterisk) within the right thyroid (*Bxii*) with no tracheal wall invasion (asterisk). (Magnification: *Bx*, ×20; *Bxi*, ×60; *Bxii*, ×60.) (*Bxiii*) Gross picture of a sh#7 8505c cells small OTC (arrow) (Magnification: ×10.) (*Bxiv* and *Bxv*) Small OTC within the right thyroid with no tracheal wall invasion (arrow and asterisk). (Magnification: *Bxiv*, ×40; *Bxv*, ×40). (*Ci*) Gross lung image from a mouse with metastatic sh control 8505c cells OTC. (Magnification: ×10.) (*Cii*) GFP excitation reveals miliary multifocal lung micrometastases. (Magnification: ×10.) (*Ciii*) H&E stain of numerous lung micrometastasis of sh control 8505c cells (arrows). (Magnification: ×60.) (*Civ*) Gross lung image from a mouse injected with sh#1 B-Raf^{V600E} 8505c cells. (Magnification: ×10.) (*Cv*) GFP excitation and (*Cvi*) H&E staing do not reveal lung micrometastasis of sh#1 8505c cells small OTC. (Magnification: *Cv*, ×10; *Cvi*, ×40.) (*Cvii*) Gross lung image (Magnification: ×10.) and (*Cviii*) H&E stain from a mouse injected with sh#7 TSP-1 8505c. (Magnification: ×20.) (*Di*) Gross image of a large OTC of 8505c cells (arrow) in mice treated with the vehicle (control group). (*Dii*) GFP excitation shows a large right OTC (arrow) with extension to the left side (control group). (*Diii*) GFP excitation reveals miliary multifocal lung micrometastases (arrows) in mice treated with vehicle (control group). (*Div*) Small OTC of 8505c cells (arrow) in mice treated with PLX4720 30 mg/kg per day for 21 days. (*Dv*) GFP excitation shows a small right mass (arrow) upon PLX4720 treatment. (*Dvi*) Significant decrease of the number of lung micrometastases in mice treated with PLX4720 (arrow). (Magnification: *Di–vi,* ×10.) *$P < 0.05$; ***$P < 0.001$.

B-Raf^{V600E} overexpression in normal human BJ fibroblasts confirmed up-regulation of TSP-1 mRNA and protein levels by B-Raf^{V600E}. BJ-B-Raf^{V600E} cells also acquired an invasive phenotype compared with controls, thus reinforcing our findings regarding the importance of B-Raf^{V600E} mutation in altering TSP-1 expression and the invasive program of the cell. By contrast, our data indicate that WT B-Raf mRNA silencing in TPC-1 cells (RET/PTC-1) does not affect TSP-1 expression levels, indicating that TSP-1 expression is regulated differently in various cell types and is dependent on genetic context.

TSP-1 has many functional domains that interact with a variety of cell surface receptors and can trigger different biological effects in a cell context-dependent manner (9, 10). The 3TSR domain plays an important role in activation of TGF-β1 in vivo (9, 10). Others are certainly involved in several processes of the ECM microenvironment (i.e., amino-terminal domain) by the binding to integrins (i.e., α3β1 or α6β1) (23), which have an important role for tumor cell migration and invasion (24, 25). Here, treatment with recombinant amino-terminal domain and to a lesser extent 3TSR resulted in restoration of invasive behavior in 8505c cells that had undergone knockdown of B-Raf^{V600E} or TSP-1. Only these TSP-1 domains were able to restore the aggressive phenotype of the 8505c cells grown in 3D cultures, implying a link between the B-Raf^{V600E} action and the amino-terminal or 3TSR domains. Our observation is supported by Chandrasekaran et al. (23), who showed a critical role for the TSP-1 amino-terminal domain in human breast cancer cell adhesion, migration, and invasion via putative binding sites for α3β1 integrin. Integrins are receptors for cellular adhesion molecules such as TSP-1 (9, 10), and they initiate "outside-in" signal transduction events that modulate gene expression, cell proliferation, migration, and invasion (26). Importantly, our GSEA analysis detected an increase in α3, α6, and β1 integrins levels in B-Raf^{V600E}-positive PTCs vs. WT B-Raf PTCs or NT (*SI Text*). B-Raf^{V600E} oncoprotein contributes to the invasive behavior of an aggressive thyroid cancer cell line in vitro, perhaps through an interaction of the amino-terminal or 3TSR domains of TSP-1 with these integrins.

We proceeded with in vivo testing of our hypothesis using an orthotopic model of thyroid cancer with 8505c cells, a unique cell line that is not cross-contaminated or redundant, harboring B-Raf^{V600E} (11), and originating from a patient with papillary thyroid carcinoma with anaplastic features (27). Our in vivo testing revealed that 8505c cells with B-Raf^{V600E} or TSP-1 knockdown resulted in significantly smaller orthotopic thyroid carcinomas and showed a dramatic decrease in the occurrence of lymph node and lung micrometastases. TSP-1 has been proposed to have both prometastatic and antimetastatic properties (9, 10). Yee et al. (9) have recently demonstrated that TSP-1 can promote metastasis to lungs in a transgenic mouse model of breast cancer. Additionally, previous in vitro studies suggested that TSP-1 promotes tumor cell adhesion, migration, and invasion (28). Interestingly, it has been

MEDICAL SCIENCES

reported that plasma TSP-1 levels are higher in patients with advanced breast cancer vs. patients with early breast cancer, and these levels are significantly higher than in normal controls (29). TSP-1 is a potent inhibitor of angiogenesis by multiple mechanisms, including direct interaction with VEGF and inhibition of MMP-9 activation (10, 30). By contrast, other activities of TSP-1 seem to promote tumor cell migration, invasion, and metastasis (10). Overall, the effects of TSP-1 on any given tumor's metastatic potential probably depends on genetic and/or epigenetic changes in the tumor cells themselves, as well as its antiangiogenic effects on endothelial cells. In our study, we found that the protein levels of some angiogenic factors (e.g., VEGF) were higher in the orthotopic thyroid tumors with B-Raf^{V600E} mutation as compared with the tumors with B-Raf^{V600E} knockdown (*SI Text*). Orthotopic thyroid carcinomas with TSP-1 knockdown showed an increase of VEGF and MMP-9 protein levels (*SI Text*). These results are consistent with the observations that TSP-1 mediates the uptake and clearance of both VEGF and MMP-9 (10).

In summary, we have identified a robust B-Raf^{V600E}-associated gene expression profile in human PTCs that includes genes that share the same function and/or signaling pathway. Our results indicate that B-Raf^{V600E} may affect tumor aggressiveness through the positive regulation of TSP-1 expression. The N-terminal domain and to a lesser extent 3TSR domain (α3β1 and α6β1 integrins-binding domains) of TSP-1 may cooperate with B-Raf^{V600E} in 8505c cells to promote tumor invasion and metastases. PLX4720, an orally available B-Raf^{V600E}-selective inhibitor displays activity against advanced human thyroid cancer in an animal model, which reproduces the clinical–pathologic behavior of this type of cancer.

Materials and Methods

Details regarding antibodies, cell culture, RNA, real-time RT-PCR, primers sequence, protein assays (Western blotting), transient transfections, lentivirus (shRNA) or retrovirus transduction, cell cycle analysis, BrdU, apoptosis, immunofluorescence, adhesion, migration, and invasion assays, 3D cell cultures, tissue microarrays, and immunohistochemistry can be found in *SI Text*.

Gene Set Enrichment Analysis. The human samples used in this study were previously analyzed using the Affymetrix HG-U133A Genechips (8). We performed GSEA (version 2.0.1) according to Subramanian et al. (7). Gene sets with a FDR of <0.2000 were considered differentially expressed. More details about GSEA and gene validation are described in *SI Text*.

Tumor Implantation and in and ex Vivo Bioimaging. All animal work was done in accordance with federal, local, and institutional guidelines. For the orthotopic tumor implantation model using sh control, sh-B-Raf^{V600E}, or sh-TSP-1 8505c human thyroid cancer cells, we used 18 (6 per group) SCID female mice (Taconic). PLX4720 was provided by Plexxikon. More details about tumor implantation, scoring for metastasis, in vivo and ex vivo bioimaging (i.e., GFP excitation), and PLX4720 are provided in *SI Text*.

Statistical Analysis. Statistical analysis was carried out using Microsoft Excel Software. Results were compared using the Student *t* test and χ^2 test. *P* values of <0.05 were considered significant (*$P < 0.05$, **$P < 0.01$, ***$P < 0.001$).

ACKNOWLEDGMENTS. We thank Dr. Yutaka Kawami (Keio University, Japan) for kindly providing the vectors HIV-U6; Dr. W.C. Hahn [Harvard Medical School (HMS)] for providing BJ cells and pLKO and pBABE constructs; Mr. Mark Duquette and James Lawler for technical assistance; Drs. Shou-Ching Shih, Michelangelo Fiorentino, Amrik Singh, and Peter Sadow for help with the real-time RT-PCR experiments, Ariol instrument SL-50, anti-tag-cmyc antibody, and MMP-9 and VEGF immunohistochemistry, respectively; Drs. Gideon Bollag and Paul Lin (Plexxikon) for providing PLX4720 and for technical assistance; and Dr. PierPaolo Pandolfi (HMS) for helpful suggestions. C.N. was a recipient of a PhD Fellowship in Experimental Endocrinology and Metabolic Diseases funded from Italy and carried out at HMS. This study was funded through National Institutes of Health Grant CA130895 (to S.P. and J.L.) and from the Massachusetts General Hospital Faculty Development Fund, Polsky Family Fund, and American Thyroid Association (S.P.).

1. National Comprehensive Cancer Network (2007) *NCCN Clinical Practice Guidelines in Oncology*. Available at http://www.nccn.org/professionals/physician_gls/f_guidelines.asp. Accessed September 16, 2009.
2. Baudin E, Schlumberger M (2007) New therapeutic approaches for metastatic thyroid carcinoma. *Lancet Oncol* 8:148–156.
3. Xing M (2007) BRAF mutation in papillary thyroid cancer: Pathogenic role, molecular bases, and clinical implications. *Endocr Rev* 28:742–762.
4. Frasca F, et al. (2008) BRAF(V600E) mutation and the biology of papillary thyroid cancer. *Endocr Relat Cancer* 15:191–205.
5. Nucera C, Goldfarb M, Hodin R, Parangi S (2009) Role of B-Raf(V600E) in differentiated thyroid cancer and preclinical validation of compounds against B-Raf(V600E). *Biochim Biophys Acta* 1795:152–161.
6. Davies H, et al. (2002) Mutations of the BRAF gene in human cancer. *Nature* 417: 949–954.
7. Subramanian A, et al. (2005) Gene set enrichment analysis: A knowledge-based approach for interpreting genome-wide expression profiles. *Proc Natl Acad Sci USA* 102:15545–15550.
8. Giordano TJ, et al. (2005) Molecular classification of papillary thyroid carcinoma: Distinct BRAF, RAS, and RET/PTC mutation-specific gene expression profiles discovered by DNA microarray analysis. *Oncogene* 24:6646–6656.
9. Yee KO, et al. (2009) The effect of thrombospondin-1 on breast cancer metastasis. *Breast Cancer Res Treat* 114:85–96.
10. Kazerounian S, Yee KO, Lawler J (2008) Thrombospondins in cancer. *Cell Mol Life Sci* 65:700–712.
11. Schweppe RE, et al. (2008) Deoxyribonucleic acid profiling analysis of 40 human thyroid cancer cell lines reveals cross-contamination resulting in cell line redundancy and misidentification. *J Clin Endocrinol Metab* 93:4331–4341.
12. Nucera C, et al. (2009) A novel orthotopic mouse model of human anaplastic thyroid carcinoma. *Thyroid* 19:1077–1084.
13. Tsai J, et al. (2008) Discovery of a selective inhibitor of oncogenic B-Raf kinase with potent antimelanoma activity. *Proc Natl Acad Sci USA* 105:3041–3046.
14. Elisei R, et al. (2008) BRAF(V600E) mutation and outcome of patients with papillary thyroid carcinoma: A 15-year median follow-up study. *J Clin Endocrinol Metab* 93: 3943–3949.
15. Kannengiesser C, et al.; EORTC Melanoma group (2008) Gene expression signature associated with BRAF mutations in human primary cutaneous melanomas. *Mol Oncol* 1:425–430.
16. Sumimoto H, et al. (2004) Inhibition of growth and invasive ability of melanoma by inactivation of mutated BRAF with lentivirus-mediated RNA interference. *Oncogene* 23:6031–6039.
17. Garraway LA, et al. (2005) Integrative genomic analyses identify MITF as a lineage survival oncogene amplified in malignant melanoma. *Nature* 436:117–122.
18. Majack RA, Mildbrandt J, Dixit VM (1987) Induction of thrombospondin messenger RNA levels occurs as an immediate primary response to platelet-derived growth factor. *J Biol Chem* 262:8821–8825.
19. Patel MK, Lymn JS, Clunn GF, Hughes AD (1997) Thrombospondin-1 is a potent mitogen and chemoattractant for human vascular smooth muscle cells. *Arterioscler Thromb Vasc Biol* 17:2107–2114.
20. Wilson KE, Li Z, Kara M, Gardner KL, Roberts DD (1999) Beta 1 integrin- and proteoglycan-mediated stimulation of T lymphoma cell adhesion and mitogen-activated protein kinase signaling by thrombospondin-1 and thrombospondin-1 peptides. *J Immunol* 163: 3621–3628.
21. Sid B, et al. (2008) Thrombospondin-1 enhances human thyroid carcinoma cell invasion through urokinase activity. *Int J Biochem Cell Biol* 40:1890–1900.
22. Montero-Conde C, et al. (2008) Molecular profiling related to poor prognosis in thyroid carcinoma. Combining gene expression data and biological information. *Oncogene* 27:1554–1561.
23. Chandrasekaran S, Guo NH, Rodrigues RG, Kaiser J, Roberts DD (1999) Pro-adhesive and chemotactic activities of thrombospondin-1 for breast carcinoma cells are mediated by alpha3beta1 integrin and regulated by insulin-like growth factor-1 and CD98. *J Biol Chem* 274:11408–11416.
24. Morini M, et al. (2000) The alpha 3 beta 1 integrin is associated with mammary carcinoma cell metastasis, invasion, and gelatinase B (MMP-9) activity. *Int J Cancer* 87:336–342.
25. Iyer V, Pumiglia K, DiPersio CM (2005) Alpha3beta1 integrin regulates MMP-9 mRNA stability in immortalized keratinocytes: A novel mechanism of integrin-mediated MMP gene expression. *J Cell Sci* 118:1185–1195.
26. Hynes RO (2002) Integrins: Bidirectional, allosteric signaling machines. *Cell* 110: 673–687.
27. Ito T, et al. (1994) Establishment of two human thyroid carcinoma cell lines (8305C, 8505C) bearing p53 gene mutations. *Int J Oncol* 4:583–586.
28. Qian X, Tuszynski GP (1996) Expression of thrombospondin-1 in cancer: A role in tumor progression. *Proc Soc Exp Biol Med* 212:199–207.
29. Byrne GJ, et al. (2007) Angiogenic characteristics of circulating and tumoural thrombospondin-1 in breast cancer. *Int J Oncol* 31:1127–1132.
30. Folkman J (1992) The role of angiogenesis in tumor growth. *Semin Cancer Biol* 3: 65–71.